Pure appl. geophys. 160 (2003) 2053–2069
0033–4553/03/112053–17
DOI 10.1007/s00024-003-2419-8

Pure and Applied Geophysics

Failure of Marine Deposits and their Redistribution by Sediment Gravity Flows

J. P. M. SYVITSKI[1] and E. W. H. HUTTON[1]

Abstract — ***SedFlux*** simulates the fill of sedimentary basins, and can be used to examine the location and attributes of sediment failure on continental margins and the runout of their associated sediment gravity flows. Numerical experiments show how the evolving boundary conditions of sea-level fluctuations, floods, storms, tectonic and other relevant processes control the rate and size of slope instabilities. By tracking deposit properties (pore pressures, grain size, bulk density, porosity), a finite-slope factor-of-safety analysis of marine deposits examines failure potential. A decider routine is used to determine whether the failed material will travel down slope as turbidity current or a debris flow. Examples provided insight into: (i) why fjords dominated by turbidity current deposition often contain debris flow deposits; (ii) how glaciated margins prograde seaward through shallow failures of low yield strength material; and, (iii) how large-scale basin subsidence can control the onset of canyon formation across continental slopes.

Key words: Sediment failure, gravity flows, numerical models.

1. Introduction

Stratigraphic simulation models (SSMs) are useful for predicting the time-varying impact of sedimentary processes, and the distribution of lithostratigraphic properties away from points of control (FRANSEEN *et al.*, 1991). The intent of this paper is to describe the general framework of ***SedFlux*** (SYVITSKI *et al.*, 1999), with particular reference to how sediment failure and sediment gravity flow routines may be used to explore the evolution of the seascapes of continental margins.

An early SSM to explore sediment failure was DELTA6 (SYVITSKI and ALCOTT, 1995). DELTA6 had delta foresets fail by oversteepening and subsequently move downslope as turbidity currents (using a non-dynamic highly parameterized scheme). Offshore slope failures were located by a finite-slope factor-of-safety (Janbu) technique. Failed sediment was transported offshore by SKRED, using a Lagrangian 1-D debris flow scheme using bilinear rheology (SYVITSKI and ALCOTT, 1995). More recently LOSETH (1999) described a SSM called DEMOSTRAT, that includes simple forms of marine sedimentation coupled to an infinite-slope stability analysis and

[1] Institute of Arctic and Alpine Research, University of Colorado at Boulder, 1560 30th Street, Campus Box 450, Boulder CO, 80309-0450, U.S.A.

rule-based gravity flow algorithms. SYVITSKI *et al*. (1999) described a beta version of 2-D ***SedFlux***-0.9F that incorporates advanced finite-slope stability analysis and fully dynamic sediment gravity flow modules. Here we describe the latest version of 2-D ***SedFlux***-1.1C with emphasis on slope stability and sediment failure experiments.

2-D ***SedFlux*** (SYVITSKI and HUTTON, 2001) simulates the lithologic character of basin stratigraphy (Fig. 1) by:

- spreading a river-delivered bedload of coarse material across the tidal range,
- dispersing the suspended sediment from the river through either surface (hypopycnal) or subsurface (hyperpycnal) plumes,
- dispersing and sorting the seafloor sediment by ocean storm events, failure of marginal deposits and their subsequent transport as sediment gravity flows (turbidity currents or debris flows),
- altering the accommodation space through thermal subsidence and tectonic displacements (formation of anticlines, synclines, growth faults, earthquake displacements, uplift), and
- compacting and preserving the sediment as a final deposit.

Recent unpublished additions include the determination of tsunami properties generated during sediment failure routines (HUTTON *et al*., 2000). In addition, ***SedFlux*** offers the ability to include other seismic and failure modules discussed in this volume. The history and details of model development can be found elsewhere (SYVITSKI *et al*., 1999; SYVITSKI and HUTTON, 2001).

*2. Overview of 2-D **SedFlux***

2-D ***SedFlux*** predicts basin stratigraphy in the horizontal and vertical direction. The initial basin geometry defines the initial bathymetry, at a user-specified horizontal resolution ($\sim$10 m). The vertical resolution is also user specified ($>$1 cm), within which deposited sediment have their characteristics averaged, except for grain size in which the entire size frequency distribution is tracked. Each of the modeled processes has its own unique resolution (temporal and spatial) independent of the ***SedFlux*** architecture.

Sediment is supplied to a basin through a single river, which has variable river mouth dynamics for each time step of the ***SedFlux*** simulation. The model river transports a multi-grain size suspended load and a single grain size bedload. Sediment enters the model domain solely through a river mouth located just upstream of a delta plain. The bedload component is deposited through stochastic processes across the delta plain and intertidal zone. The river's suspended sediment load is discharged as a surface plume, or as a hyperpycnal flow, depending upon the sediment-laden density of the river water.

Ocean energy is allowed to vary in intensity throughout the year, and can rework the seafloor, depending upon the strength of a particular storm, water depth, and

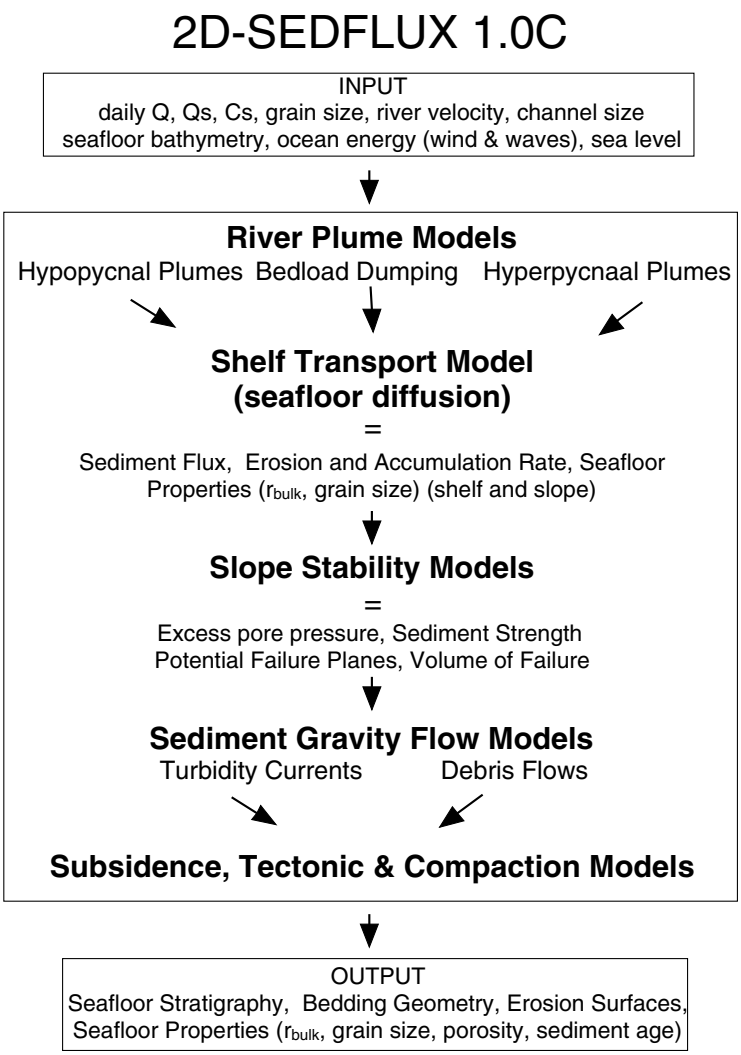

Figure 1
Flow chart of 2-D ***SedFlux*** version 1.1C, showing inputs, ***SedFlux*** model components, and outputs (modified from SYVITSKI and HUTTON, in press). Symbols include Q = water discharge, Qs = sediment discharge, and Cs = sediment concentration.

grain size properties of the seafloor. Sediment lags may locally develop and armor finer-grained material, preventing it from being winnowed away. Sediment failure occurs if potential failure planes are found to be unstable. Failed material is transported downslope as a turbidity current or as a debris flow.

Sea-level and base level are adjusted for each domain node (bin) at each time step. In this manner a eustatic sea-level curve can be used to control ocean level,

while base level changes resulting from subsidence or tectonic causes can work to modify the eustatic curve into a local relative sea-level curve. Faulting is user-controlled as either progressive (i.e., for a growth fault) or stepped motion of the bedrock. The river erodes material uplifted on land over time, and the eroded material is transported either as bedload or suspended load, depending on its size characteristics. Details regardings the physics and the numerics of each of the individual processes can be found in SYVITSKI and HUTTON (2001) and references therein.

3. Sediment Failure Routine in *SedFlux*

The failure of continental margin sediment and its subsequent movement plays an important role in transferring sediment into deeper water. Because ***SedFlux*** is designed to simulate the fill of sedimentary basins which have complex bathymetric shapes, a finite-slope stability routine is considered to be most appropriate. The geometry and location of failures are determined using the Janbu factor-of-safety analysis with the method of slices (ANDERSON and RICHARDS, 1987). The Janbu method is useful for the analysis of noncircular slip surfaces. The method ignores interslice forces, although a technique is available to correct for these forces (ANDERSON and RICHARDS, 1987). Interslice forces are invariably small, adjusting the calculated factor of safety by less than 10%, depending on the geometry of the problem as well as the soil conditions.

SedFlux examines a series of possible elliptical failure surfaces for stability (Fig. 2). The static stability of a possible failure plane is characterized through its factor of safety as,

$$F_{\text{total}} = \frac{\sum_{i=0}^{n} \left[b_i \left(c_i + \left(\frac{W_i}{b_i} - u_i \right) \tan \phi_i \right) \frac{\sec \alpha_i}{1 + \frac{\tan \alpha_i \tan \phi_i}{F_{\text{total}}}} \right]}{\sum_{i=0}^{n} W_i \sin \alpha_i} \tag{1}$$

where b is the width of a slice, c is the cohesion of the sediment, W is the weight per unit depth of the sediment, u is the excess pore pressure, ϕ is the sediment friction angle, α is the slope of the failure surface, and F_{total} is the factor of safety for the entire failure (with iterative convergence to a solution).

W is mass (M) of the sediment column times the acceleration due to gravity (g), therefore to include earthquake forces associated with ground acceleration (A_g), then $W = M\ (g + A_g)$. During an earthquake, a seismic wave exerts an additional body force on a deposit. Therefore, an earthquake probability frequency distribution (i.e., earthquake intensity as measured at the slip plane versus return interval) is used to explore dynamic slope stability. For such a scenario, associated ground acceleration (A_g) is acquired for each stability analysis performed in a simulation (typical values of A_g range from 0 to $0.3g$). Thus an earthquake reduces the factor of safety,

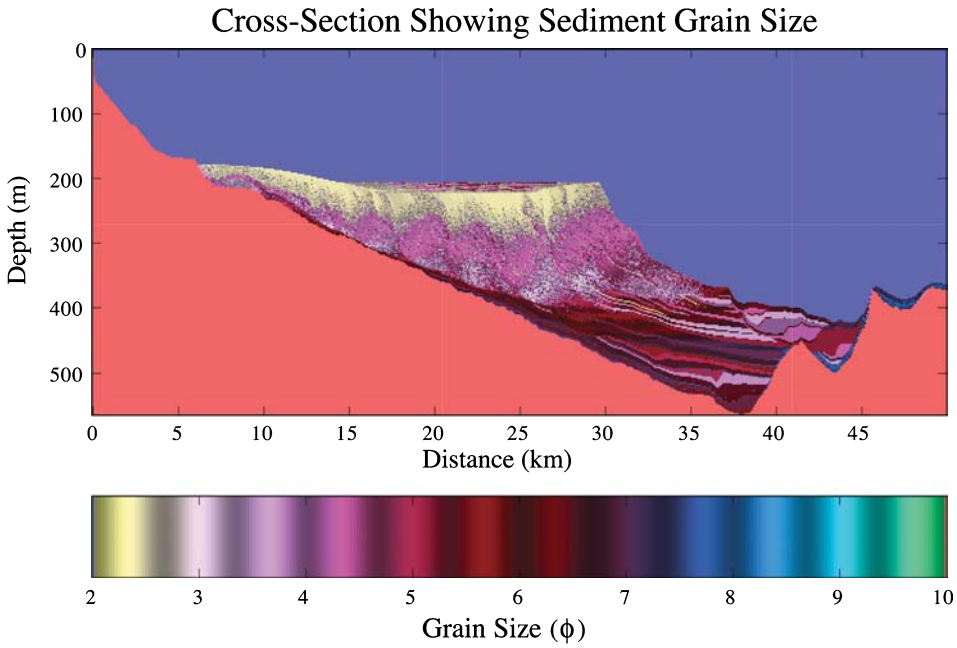

Figure 2
A 2-D ***SedFlux*** simulation of Knight Inlet, showing the sediment accumulation in terms of grain size. Distances and depths are from the beginning of the numerical model domain. Seafloor slopes were examined by FAIL subroutine and thirty-five mass failure events were generated in the 12,000-yr period; many more delta front failures due to foreset oversteepening shed low concentration turbidity currents. The 35-slope failures formed into debris flows (seen as layers of uniform grain size). The turbidites are found to be very thin bedded and graded sediment layers. Sea-level fell and rose during the simulation experiment (after MOREHEAD *et al*., 2001).

increasing the likelihood of slope failure. WILSON and KEEFER (1983) provide another comparable method of introducing ground accelerations to a factor of safety analysis. Neither method, however, includes the contribution of water pressures generated by the earthquake itself, although in principle ***SedFlux*** could also be configured to include that phenomenon.

The excess pore pressure is obtained from consolidation theory under the assumption that these excess pressures are entirely the result of trapping pore water while compacting fine-grained sediment of low permeability. Using Gibson's graphical approximation (1958), we find

$$u_i = \frac{\gamma' z_i}{a_i} \quad , \tag{2}$$

where γ' is the submerged specific weight of the sediment $(\gamma' = \gamma - \gamma_f)g$, and z is the depth of the failure plane with respect to the seafloor. The variable a is given through the relation,

$$a \equiv 6.4\left(1 - \frac{T}{16}\right)^{17} + 1 \quad , \tag{3}$$

where T is a constant defined as,

$$T \equiv \frac{m^2 t}{C_v} \quad , \tag{4}$$

where m is sedimentation rate, t is the time for deposition, and C_v is the consolidation coefficient for the sediment. If the static factor of safety is found to be less than some threshold, then the sediment is failed and moved downslope as a sediment gravity flow, otherwise it is deemed to be stable. The width of the submarine landslide is scaled to be 0.25 times the length of the failure. The Janbu method neglects the influence of fractures, although in principle ***SedFlux*** could be configured to include that phenomenon.

4. The Mass Flow Decider

In ***SedFlux***, once a failed mass is identified, the properties of the deposit are examined. If the failed material is clayey (user-defined, e.g., >10% clay), then the failed sediment mass is transported down-slope as a debris flow. An appropriate clay content is used as a proxy for ensuring low hydraulic conductivity and low permeability and thus the generation of a debris flow (MOHRIG *et al.*, 1999). This ensures that a viscoplastic (Bingham) rheology is achieved (ELVERHØI *et al.*, 2000). As outlined below, our modeled dynamics does not allow for the debris flow to erode the seafloor. Thus the grain size of the final deposit is equal to the homogenized grain size of the initial failed sediment mass.

If the material is sandy or silty, with little clay (user-defined, e.g., <10% clay) then the failed sediment mass is transported down-slope as a turbidity current. If the material moves as a turbidity current, flow accelerations may cause erosion of the seafloor and this entrained sediment may increase the clay content of the gravity flow compared to the initial failed sediment mass. Deposition of sand and silt along the flow path may result in the turbidity current transporting primarily clay in the distal reaches along the flow path (SKENE *et al.*, 1997).

5. Turbidity Currents

In 2-D ***SedFlux*** 1.1C, turbidity currents are initiated at the river mouth as a hyperpycnal flow, or from a slope failure located somewhere in the offshore, as allowed by the above decider routine. In the case of a slope failure, the failed mass does not transform directly into a turbidity current, rather the initial concentration

of the gravity flow is set below some user-defined value less than the Bagnold limit (9% concentration by volume: MULDER *et al.*, 1997). Using this initialized concentration, flow height is established and gravity pulls the current down across the seafloor, while entraining water and sediment into the flow, depending on the dynamics associated with the evolving boundary conditions. Friction around and within the flow work to slow the flow, until all momentum is consumed.

Different turbidity current subroutines within ***SedFlux*** are available. INFLO is briefly reviewed here, but BANG is also available. BANG1D is 1-D, layer-averaged, and based on the Lagrangian form of the equations for the conservation of fluid, sediment, momentum and turbulent kinetic energy in a turbidity current (PRATSON *et al.*, 2000, 2001).

INFLO is a psuedo-2-D layer-averaged (specified but variable width), turbidity current model, configured in the Eulerian steady-state form, employing the conservation of fluid, sediment, and momentum. INFLO uses an internal friction parameterization and drag coefficient terms to close the solution (SKENE *et al.*, 1997; MULDER *et al.*, 1997). A turbidity current contains particles in suspension supported by fluid turbulence but maintaining enough of a sediment density that a gravitational driving force is produced that accelerates the flow downslope as a mixture of sediment and water. Energy is lost from friction of the flow across the seafloor, from friction beneath an overlying water mass, and from friction within the flow (grain-grain interaction). The balance of these terms is expressed as,

$$\frac{\partial U}{\partial t} = g_0 \sin(\beta C) - \frac{E + C_d}{h} U^2 - g_0 \left(\frac{eC - 1}{e - 1} \right) \cos(\beta C) \tan \phi \quad , \tag{5}$$

where, U is vertically integrated downslope velocity, g_0 is reduced gravity equal to $g(\rho_s - \rho)/\rho, \beta$ is slope, E is entrainment coefficient, C_d is drag coefficient, h is flow thickness, ρ is ambient fluid density, ρ_f is density of the flow, ρ_s is grain density, ϕ is angle of internal friction, C is bulk volume concentration of sediment calculated for each grain size, and g is acceleration due to gravity.

As the flow travels it entrains sea water and flow volume is increased. Fluid continuity is:

$$\frac{\partial Q}{\partial x} = EUW_F \quad , \tag{6}$$

where W_F is width of the flow (i.e., width of submarine canyon or basin floor), Q is volume discharge, x is distance in the downslope direction, and E is the entrainment coefficient that relates the amount of seawater that is entrained by flow.

Sediment can enter and exit the flow. As the flow falls below some critical velocity, sediment begins to be deposited. Above some critical shear stress, sediment from the seafloor is eroded and entrained into the flow. The continuity equation for suspended load is:

$$\frac{\partial J_i}{\partial x} = E_R - D_R = \left[\left(\frac{C_d \rho_f U^2 - \sigma_b}{\sigma_a}\right)\frac{\varphi_i W_F}{\text{day}}\right] - D_R \ , \tag{7}$$

where E_{Ri} is the rate of erosion averaged over one day of the i-th grain size of the seafloor, day is 86,400 s, σ_a is the gradient in the shear strength of the seafloor sediment, σ_b is the shear strength of the sediment at the seafloor, and D_{Ri} is the rate of deposition of the i-th grain size,

$$D_R = \begin{cases} 0 & \text{if } U > U_{cr} \\ \dfrac{\lambda_i J_i}{U}\left(1 - \dfrac{U^2}{U_{cr}^2}\right) & \text{if } U \le U_{cr} \end{cases} \ , \tag{8}$$

and U_{cr} the critical velocity for deposition is given by,

$$U_{cr} = w_s \Big/ \sqrt{C_d} \ , \tag{9}$$

where w_s is the settling velocity of the i-th grain size.

INFLO uses a drag coefficient in three separate equations: (i) drag on the upper body of the turbidity current influencing the rate of entrainment (5); (ii) drag on the lower part of the flow linked to seafloor erosion (7); and, (iii) drag on settling particles, controlling the critical velocity of deposition (9).

6. Debris Flows

Debris flows are modeled after the properties of a Bingham plastic (viscoplastic) fluid, where deformation is driven by the excess of stress beyond the yield stress (JIANG and LEBLOND, 1992; PRATSON *et al.*, 2000; IMRAN *et al.*, 2001). The model neglects the tangential stress acting on the water-mud interface, because the viscosity of water is much smaller than that of the mud, and the basal shear of the mudflow is much greater than the interfacial shear (LIU and MEI, 1989). In addition, there is a no slip condition on the slide bottom.

The governing equations of the Lagrangian form of the depth-averaged debris flow equations, including both viscous and plug flow regions, are:

Continuity:

$$\frac{\partial D}{\partial t} + \frac{\partial}{\partial x}\left[U_p D_p + \frac{2}{3} U_p D_s\right] = 0 \ . \tag{10}$$

Momentum (shear layer):

$$\begin{aligned} &\frac{2}{3}\frac{\partial (U_p D_s)}{\partial t} - U_p \frac{\partial D_s}{\partial t} + \frac{8}{15}\frac{\partial\left(U_p^2 D_s\right)}{\partial x} - \frac{2}{3} U_p \frac{\partial (U_p D_s)}{\partial x} \\ &\quad = D_s g\left(1 - \frac{\rho_w}{\rho_m}\right) S - D_s g \frac{\partial D}{\partial x} - 2\frac{\mu}{\rho_m}\frac{U_p}{D_s} \ . \end{aligned} \tag{11}$$

Momentum (plug flow layer):

$$\frac{\partial(U_p D_p)}{\partial t} + \frac{\partial\left(U_p^2 D_p\right)}{\partial x} + U_p \frac{\partial D_s}{\partial t} + \frac{2}{3} U_p \frac{\partial(U_p D_s)}{\partial x} = D_p g \left(1 - \frac{\rho_w}{\rho_m}\right) S - D_p g \frac{\partial D}{\partial x} - \frac{\tau_y}{\rho_m} \quad , \tag{12}$$

where D is the total depth of the debris flow ($D_p + D_s$); D_p and U_p are the depth and layer-averaged velocity of the upper plug zone, respectively; D_s and U_s are the depth and layer-averaged velocity of the lower shear layer, respectively; g is acceleration due to gravity; S is slope; ρ_w is density of ocean water; ρ_m is density of the mud flow; τ_y is yield strength, and μ is kinematic viscosity. The yield strength controls how the deposit is stretched out. We typically use values of 100 Pa, but higher values will allow the debris flow to flow downslope more as a block then as a flow.

7. Application of 2-D ***SedFlux*** 1.1C to Slope Stability Studies

Our first example is from a 12,000-yr simulation of the sediment architecture forming Knight Inlet, a fjord in British Columbia, where the seafloor slopes are examined by the FAIL subroutine (Fig. 2; MOREHEAD *et al.*, 2001). Knight Inlet is a basin that is annually subjected to numerous gravity-flow events (MOREHEAD *et al.*, 2001). A river introduced a variable sediment load into the basin every day. An initial dropping relative sea-level (due to isostatic rebound as the glaciers retreated) and then a slow rise in relative sea-level (due to rising eustatic sea-level) was imposed on the simulated basin. Numerous small failures, near the delta foresets, generated turbidity currents that deposited their sandy load along the proximal part of the pro-delta slope (Fig. 2). Thirty-five large slope failures were initiated using the Janbu finite-slope factor-of-safety analysis (Fig. 2). Failure lengths ranged between 600 m and 3800 m, all were located in muddy facies on rather steep slopes (2° to 3.4°). The failure planes reached depths in the sediment column of 8 m to 30 m (Fig. 2). The failed sediment masses moved as debris flows, with run out distances of between 5 and 21 km. This situation of rarer debris flows mixed with numerous turbidity current events is common to fjord environments (HEIN and SYVITSKI, 1992; SYVITSKI and LEE, 1997).

The second simulation example is from a prograding margin fed with clayey sediment from an ice sheet and thus dominated by the deposition from debris flows (Fig. 3). Numerous slope failures occur near the shelf-slope break and the failed sediment masses moved as debris flows, depositing their sediment load along the length of the slope. Debris flow lobes accumulate near the base of the continental slope (Fig. 3B). Debris flow-dominated margins are common along glaciated and polar margins, where the sedimentary feed is via clayey basal till (VORREN *et al.*, 1998; ELVERHØI *et al.*, 1997). The ***SedFlux*** simulation can be compared with a

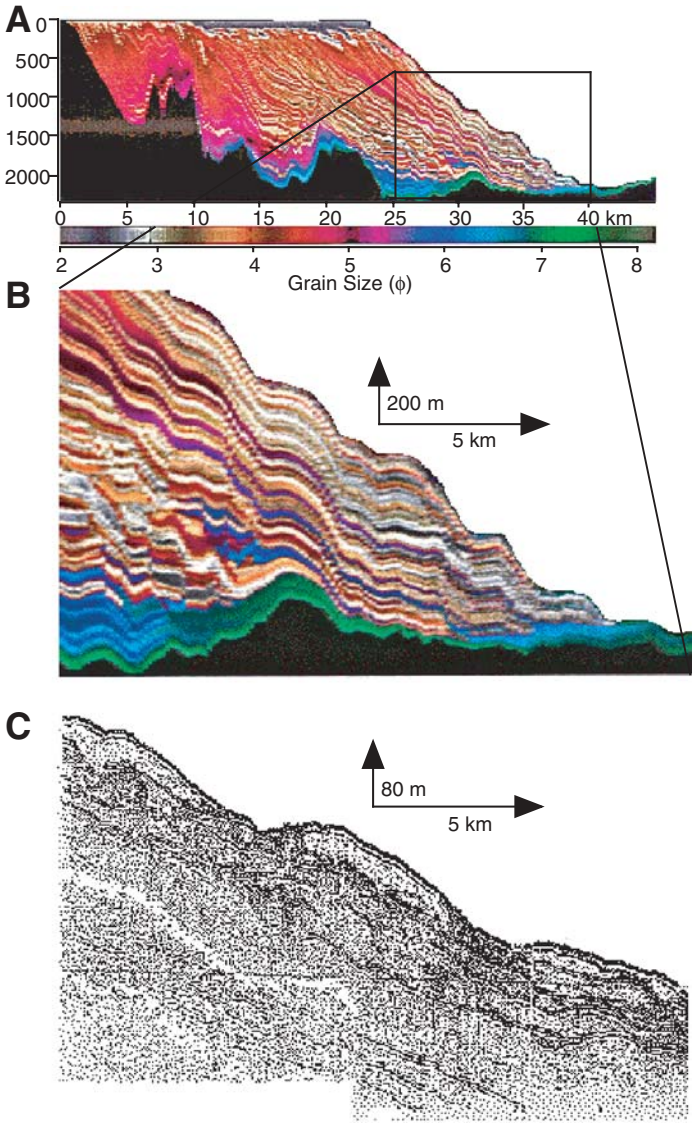

Figure 3

(A) A 2-D ***SedFlux*** run of a prograding debris flow-dominated margin. Numerous slope failures occur near the shelf-slope break and associated debris flows deposit their sediment load along the length of the slope. (B) Close-up of the amalgamation of debris flow lobes near the base of the continental slope. (C) 10-cubic inch Sleeve-Gun seismic record collected on HU93-030 off of the Kangerlussuaq Fan, East Greenland (for details on this record see STEIN and SYVITSKI, 1997). Debris flow lenses show characteristic transparent or chaotic internal reflections.

seismic record collected off of the Kangerlussuaq Fan, East Greenland (Fig. 3C, for details on this record see STEIN and SYVITSKI, 1997). Debris flow lenses show characteristic transparent or chaotic internal reflections.

A reasonable question arising from a comparison of our first and second examples would be why some debris flows produce thick deposits on the basin floor (i.e., Fig. 2), whereas other debris flows deposit their load along the entire length of a continental slope, stretched and thin (i.e., Fig. 3)? The answers lies among four parameters: failure size, steepness of the flow path (i.e., steepness of the continental slope), length of the runout path down a continental slope, and the yield strength of the failed material. If the failure size is small, the driving force (submerged failure weight) is concomitantly small and thus there is a tendency for sediment to deposit nearer the point of failure. If the flow path is steep, then there is a tendency for sediment to be deposited far from its point of failure, often near the slope-rise break. If the yield strength is low, there is a tendency for the deposit to stretch out. If the flow path is long, sediment will be more often retained on the continental slope. Thus the conditions for debris flows to deposit on the continental slopes of glaciated margins (Fig. 3) include numerous small failures of initial deposits possessing relatively low yield strengths, where debris flows travel across a relatively long and gentle slope. DIMAKIS *et al*. (2000) have used a similar analysis to explain the progradation of the Svalbard-Barents Sea margin.

Our third example (Fig. 4) is used to show how the *decider routine* works. Three 2000-year simulations are provided of a river delta prograding into an idealized margin. In each case, the exact sediment input to the numerical model (river system) is used. Sea-level is held constant. Sediment accumulates on a 0.75° slope over the first 25-km section of the basin, then the basin flattens outs at a water depth of 430 m. Less than 20% of the sediment discharged by the river is sand, the remainder is silt and clay. The river bedload is spread out over ~1 km distance from the river mouth, providing for steep foresets of muddy sand.

In the first realization (Fig. 4A), the decider is set to have failed sediment masses move seaward as a debris flow if the averaged grain size of the material is ≥10% clay. Many debris flow deposits can be seen and most of them have petered out at the base of the prodelta slope with little spillage onto the flat basin floor. Close to 50 debris flows were generated of a variety of size and grain size characteristics. Minimal turbidite deposits were generated (a small thin deposit can be seen at the 120 km location position). In the second realization (Fig. 4B), debris flows were only generated if the averaged grain size of the material is ≥20% clay. As a result there is a 66% decrease in debris flow generation and a concomitant increase in turbidity currents. The latter flowed out onto the basin floor, travelling tens of kilometers and depositing their load as thin bedded, vertically and laterally graded turbidites. In the third realization (Fig. 4C), no debris flows were generated as the criteria was set to ≥40% clay. Therefore all failed material was transported as turbidity currents. Turbidity current-dominated margins (Fig. 4C) give rise to steeper marginal slopes in

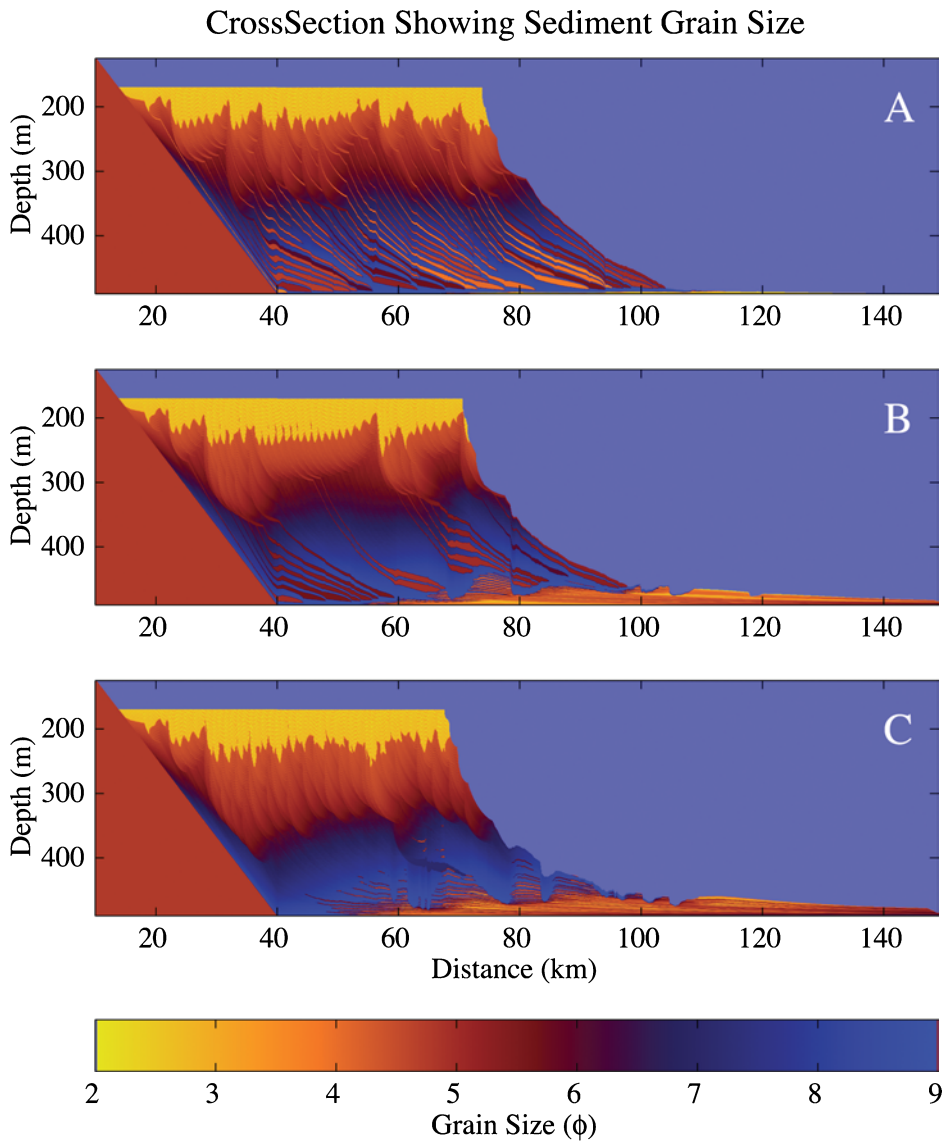

Figure 4

Three realizations of a deepwater deltaic margin prograding over a 3/4° slope onto a flat basin floor. The realizations show how ***SedFlux*** can use the grain size of the failed sediment mass to control the generation of debris flows and turbidity currents. In (A) the decider is set to have failed sediment masses move seaward as a debris flow if the averaged grain size of the material is ≥10% clay. The criterion changes to ≥20% clay in (B) and ≥40% clay in (C). As a consequence all failed sediment masses were translated as debris flows in (A) and as turbidity currents in (C), with the (B) realization falling some place in between. See text for details.

contrast to debris flow-dominated margins (Fig. 4A). The steeper slopes cause the turbidity currents to ignite and this in turn increases the rate older seafloor deposits are eroded, including older turbidite beds on the lower slope.

Our last example is using ***SedFlux*** to isolate the feedback of single process (crustal subsidence) on the formation of sediment failures near the shelf-slope break (Fig. 5). Subsidence is controlled by the sediment load (SYVITSKI and HUTTON, 2001). The model run simulates the growth of an unnamed NW Australian passive margin, using over 200,000 time steps, with the sediment input scaled to the Quaternary time period. Sea-level fluctuates 100 ± 20 m, through six separate episodes. The impact of subsidence includes development of accommodation space, thus providing the

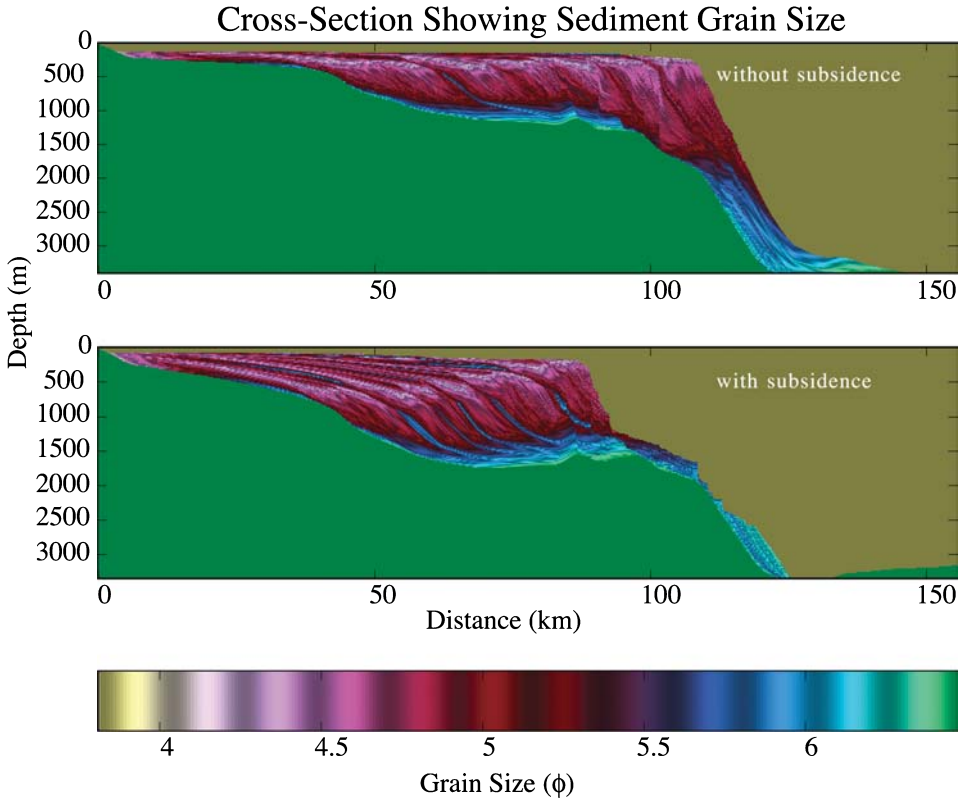

Figure 5

Formation of sediment failures near the shelf-slope break under different progradation-aggradation scenarios, as modeled by 2-D ***SedFlux***. The model run simulates a basin fill with over 200,000 time steps, and sediment input scaled to the Quaternary time period. Sea-level fluctuations were 100 m ± 20 m through six separate episodes. In simulation (A), subsidence was turned off. (B) provides a similar simulation except subsidence was turned on. Increased accommodation space associated with subsidence limits progradation of the coastline. Submarine canyons formed at the 120-km position in simulation (B) are exposed, yet in simulation (A) large canyons did not form and others are infilled (after SYVITSKI and HUTTON, 2001).

Table 1

Symbol list

Notation	Description	Unit
α	Slope of failure surface	[–]
β	Slope of the seafloor	[–]
ϕ	Angle of internal friction [sediment friction angle]	[–]
γ	Submerged density of sediment	$[ML^{-3}]$
φ	Volume concentration of *i*-th grain size in seafloor	[–]
ρ	Density of the ambient fluid	$[ML^{-3}]$
ρ_f	Density of the flow	$[ML^{-3}]$
ρ_s	Density of the sediment grain	$[ML^{-3}]$
σ_a	Shear strength vertical gradient in seafloor sediments	$[ML^{-2}T^{-2}]$
σ_b	Shear strength of sediment at the seafloor	$[ML^{-1}T^{-2}]$
A	Variable (equation 3)	[–]
A_g	Horizontal ground acceleration from an earthquake	$[LT^{-2}]$
B	Width of a slice in a failure	[L]
c	Sediment cohesion	$[MT^{-2}]$
C	Vertically averaged flow concentration	[–]
C_d	Drag coefficient	[–]
C_v	Consolidation coefficient	$[L^2T]$
D_{R_i}	Rate of deposition of the *i*-th grain size	$[LT^{-1}]$
E	Entrainment coefficient	[–]
E_{R_i}	Rate of erosion of the *i*-th grain size	$[LT^{-1}]$
F_{total}	Factor of safety for a sediment failure	[–]
G_0	Reduced gravity	$[LT^{-2}]$
H	Height of the flow	[L]
J	Flux of the *i*-th grain size between elements	$[L^3T^{-1}]$
M	Sedimentation rate	$[LT^{-1}]$
M	Mass of a column of sediment	[M]
Q	Volume discharge between flow elements	$[L^3T^{-1}]$
T	Time	[T]
T	Variable (equation 4)	[–]
U	Excess pore pressure	$[ML^{-1}T^{-2}]$
U	Vertically averaged flow velocity	$[LT^{-1}]$
U_{cr}	Critical velocity for deposition	$[LT^{-1}]$
W	Weight per unit depth of sediment	$[MT^{-2}]$
W_F	Flow width	[L]
w_s	Settling velocity	$[LT^{-1}]$
X	Horizontal position	[L]
Z	Depth of failure plane with respect to the seafloor	[L]

burial of low sea-level coastal sand bodies on the continental shelf, and the reduction in continental slope sediment accumulation. Increased accommodation space associated with the ongoing subsidence limits progradation of the coastline in the first model run (Fig. 5A). Submarine canyons formed at the 120 km position are exposed (Fig. 5A). Yet when modeled without the feedback of load-dependent subsidence, large canyons did not form and smaller canyons appear infilled (Fig. 5B). Similar scenarios have been used to explain the morphology of passive continental margins (O'GRADY *et al.*, 2000).

8. Summary

2-D ***SedFlux*** version 1.1C provides the marine geotechnical community with a new tool in understanding the complex feedbacks between marine failure and erosion and deposition by sediment gravity flows. 2-D ***SedFlux*** contains many of the important processes that distribute sediment in a marine marginal setting to form a sedimentary architecture. 2-D ***SedFlux*** can be used to investigate new numerical expressions of slope stability or mass gravity subroutines. For example we have tested two versions of debris flow models to see how differences in numerical representations and theory can result in slightly different run out lengths and deposit shapes (SYVITSKI *et al.*, 1999). Various turbidity current models (1-D, 2-D; Eulerian; Lagrangian) are presently in the process of being tested.

Results from ***SedFlux*** simulations support field observation on why fjords contain many turbidites intermixed with rarer debris-flow deposits. The high sedimentation rate environment of the steep and clay-poor foresets gives rise to numerous small failures that result in turbidity current deposition. Infrequent but large failures of the clayey prodelta environment produce debris flows that deposit their load on the basin floor. ***SedFlux*** simulations also capture how glaciated margins prograde seaward through numerous shallow failures of low yield-strength deposits at the shelf-slope break. The clay-rich sediment (till) moves downslope as debris flows depositing their load along the long run out distance of the continental slope. Finally, ***SedFlux*** simulations show how large-scale basin subsidence can affect the onset of canyon formation across continental slopes.

New upgrades to the model include the prediction of the tsunami distributions derived from landslides (HUTTON *et al.*, 2000).

Acknowledgments

We thank our geotechnical-modeling contributors: Jane Alcott, Homa Lee, Gary Parker, Lincoln Pratson, Phil Watts, J. Locat, and Jeff Wong. We are grateful for the strong encouragement of the Office of Naval Research under the MG&G management of Dr. Joseph Kravitz. This manuscript forms a contribution to ONR's STRATAFORM project under the coordination of Dr. Charles Nittrouer.

References

ANDERSON, M. G. and RICHARDS, K. S., *Slope Stability: Geotechnical Engineering and Geomorphology* (New York, John Wiley & Sons 1987).

BOOTH, J. S., SANGREY, D. A., and FUGATE, J. K. (1985), *A Nomogram for Interpreting Slope Stability of Fine-grained Deposits in Modern and Ancient Environments*, J. Sedimentary Petrology *55*, 29–36.

CARUCCIO, F. T., *Stratigraphic and geochemical controls on the occurrence of acidic mine waters and predictive technologies*. In *Quantitative Dynamic Stratigraphy* (T. A. Cross, ed.) (Prentice-Hall, N.Y. 1989) pp. 581–588.

DIMAKIS, P., ELVERHØI, A., HØEG, K., SOLHEIM, A., HARBITZ, C., LABERG, J. S., VORREN, T. O., and MARR, J. (2000), *Submarine Slope Stability on High-latitude Glaciated Svalbard-Barents Sea Margin*, Marine Geology *162*, 303–316.

ELVERHØI, A., NOREM, H., ANDERSEN, E. S., DOWDESWELL, J. A., FOSSEN, I., HAFLIDASON, H., KENYON, N. H., LABERG, J. S., KING, E. L., SEJURP, H. P., SOLHEIM, A., and VORREN, T. O. (1997), *On the Origin and Flow Behaviour of Submarine Slides on Deep-sea Fans along the Norwegian-Barents Sea Continental Margin*, Geo-Marine Lett. *17*, 119–125.

ELVERHØI, A., HARBITZ, C. B., DIMAKIS, P., MARR, J., MOHRIG, D., and PARKER, G. (2000), *On the Dynamics of Subaqueous Debris Flows*, Oceanography, *13*, 109–117.

FRANSEEN, E. K., WATNEY, W. L., KENDALL, S. G., and ROSS, W. (1991), *Sedimentary Modeling: Computer Simulation and Methods for Improved Parameter Definition*, Kansas Geolog. Survey Bull. *233*, 524 pp.

GIBSON, R. E. (1958), *The progress of consolidation in a clay layer increasing in thickness with time*. Géotechnique *8*, 171–182.

HEIN, F. J. and SYVITSKI, J. P. M. (1992), *Sedimentary Environments and Facies in an Arctic Basin, Itirbilung Fiord, Baffin Island, Canada*, Sedimentary Geology *81*, 1–29.

HUTTON, E. W. H., WATTS, P., and SYVITSKI, J. P. M. (2000), *Tsunami Generation during the Growth of a Continental Margin*, AGU 2000 Fall meeting EOS Supplement *81*(48), F649.

IMRAN, J., HARFF, P., and PARKER, G. (2001), *A Numerical Model of Submarine Debris Flow with Graphical User Interface*, Computers and Geoscience, *27*(6), 717–730.

JIANG, L. and LEBLONDE, P. H. (1992), *The Coupling of a Submarine Slide and the Surface Waves which it Generates*, J. Geophys. Res. *97*(C8), 12,731–12,744.

LIU, K. F. and MEI, C. C. (1989), *Slow Spreading of a Sheet of Bingham Fluid on an Inclined Plane*, J. Fluid Mechanics *207*, 505–529.

LOSETH, T. M. (1999), *Submarine Massflow Sedimentation: Computer Modelling and Basin Fill Stratigraphy*, Springer Lecture Notes in Earth Science *82*, 156 pp.

MARTINEZ, P. A. and HARBAUGH, J. W. (1993), *Simulating Nearshore Environments*, Computer Methods in Geosciences, Pergamon Press, *12*, 265 pp.

MOREHEAD, M. D., SYVITSKI, J. P. M., and HUTTON, E. W. H. (2001), *The Link between Abrupt Climate Change and Basin Stratigraphy: A Numerical Approach*, Global and Plantetary Change *28*, 115–135.

MORHIG, D., ELVERHØI, A., and PARKER, G. (1999), *Experiments on the Relative Mobility of Muddy Subaqueous and Subaerial Debris Flows, and their Capacity to Remobilize Antecedent Deposits*, Marine Geology *154*, 117–129.

MULDER, T., SYVITSKI, J. P. M., and SKENE, K. (1997), *Modelling of Erosion and Deposition by Sediment Gravity Flows Generated at River Mouths*, J. Sedimentary Res. *67*(3), 571–584.

NITTROUER, C. A. and KRAVITZ, J. H. (1996), *STRATAFORM: A Program to Study the Creation and Interpretation of Sedimentary Strata on Continental Margins*, Oceanography *9*(3), 146–152.

NITTROUER, C. A. (1999), *STRATAFORM: Overview of its Design and Synthesis of its Results*, Marine Geology *154*(1–4), 3–12.

O'GRADY, D. B., SYVITSKI, J. P. M., PRATSON, L. F., and SARG, J. F. (2000), *Categorizing the Morphologic Variability of Siliciclastic Passive Continental Margins*, Geology *28,* 207–210.

PRATSON, L., IMRAN, J., PARKER, G., SYVITSKI, J. P. M., and HUTTON, E. W. H. (2000), D*ebris flow versus turbidity currents: A modeling comparison of their dynamics and deposits*. In A. Bouma (ed.), *AAPG Special Publication*. 57–71.

PRATSON, L., IMRAN, J., HUTTON, E. W. H., PARKER, G., and SYVITSKI, J. P. M. (2001), *BANG1D: A One-dimensional, Lagrangian Model of Subaqueous Turbid Clouds*, Computers and Geosciences *27*(6), 701–716.

ROBINSON, A. R., LERMUSIAUZ, P. F. J., and QUINCY SLOAN III, N. (1998), *Data Assimulation*. In *The Sea: Volume 10 – The Global Coastal Ocean: Processes and Methods* (K. H. Brink and A. R. Robinson, eds.) (John Wiley and Sons, New York 1998) pp. 541–594.

SCHÄFER-NETH, C. and STATTEGGER, K., *Icebergs in the North Atlantic: Modeling circulation changes and glacio-marine deposition*. In *Computerized Modeling of Sedimentary Systems* (J. Harff, W. Lemke and K. Stattegger, eds.) (Springer, New York 1999) pp. 63–78.

SHELTON, J. L. and CROSS, T. A., *The influence of stratigraphy in reservoir simulation*. In *Quantitative Dynamic Stratigraphy* (T. A. Cross, ed.) (Prentice-Hall, N.Y. 1989) pp. 589–600.

SKENE, K., MULDER, T., and SYVITSKI, J. P. M. (1997), *INFLO1: A Model Predicting the Behaviour of Turbidity Currents Generated at a River Mouth*, Computers and Geoscience *23*(9), 975–991.

STEIN, A. B. and SYVITSKI, J. P. M., *Glaciation-influenced debris flow deposits: East Greenland slope*. In *Glaciated Continental Margins: An Atlas of Acoustical Images* (T. W. Davies, T. Bell, A. Cooper, H. Josenhans, L. Polyak, A. Solheim, M. Stoker and J. Stravers, eds.) (Chapman and Hall, London 1997) pp. 134–135.

SYVITSKI, J. P. M. and ANDREWS, J. T. (1994), *Climate Change: Numerical Modelling of Sedimentation and Coastal Processes, Eastern Canadian Arctic,* Arctic and Alpine Research *26*(3), 199–212.

SYVITSKI, J. P. M. and ALCOTT, J. M. (1995), *DELTA6: Numerical simulation of basin sedimentation affected by slope failure and debris flow runout*. In *Proceedings of the ''Pierre Beghin'' International Workshop on Rapid Gravitational Mass Movements*, 305–312, CEMAGREF, Grenoble, France.

SYVITSKI, J. P. M. and HUTTON, E. W. H. *SEDFLUXIOC: An advanced process – response numerical model for the fill of marine sedimentary basins*. Computers and Geoscience *27*(6), 731–754.

SYVITSKI, J. P. and LEE, H. J. (1997), *Sequence Stratigraphy of Lake Melville, Labrador, during Ice-sheet Retreat Since 10,000 Years BP*, Marine Geology *143*, 55–80.

SYVITSKI, J. P., PRATSON, L., and MOREHEAD, M. (1997), *EARTHWORKS: A Large Spatial Scale Numerical Model to Study the Flux of Sediment to Ocean basins and Reworking of Deposits over Various Time Scales*, AGU 1997 Fall Meeting EOS Suppliment *78*(46), F258.

SYVITSKI, J. P. M., MOREHEAD, M., and NICHOLSON, M. (1998), *HYDROTREND: A Climate-driven Hydrologic-transport Model for Predicting Discharge and Sediment to Lakes or Oceans,* Computers and Geoscience *24*(1), 51–68.

SYVITSKI, J. P. M., PRATSON, L., and O'GRADY, D. (1999), *Stratigraphic predictions of continental margins for the navy parameterizations*. In *Numerical Experiments in Stratigraphy: Recent Advances in Stratigraphic and Computer Simulations* (J. W. Harbaugh, L. W. Whatney, E. Rankay, R. Slingerland, R. Goldstein and E. Franseen, eds.). SEPM Special Publication *62*, 219–236.

TETZLAFF, D. M. and HARBAUGH, J. W. (1989), *Simulating Clastic Sedimentation* (Van Nostrand Reinhold, New York) 202 pp.

VORREN, T. O., LABERG, J. S., BLAUME, F., DOWDESWELL, J. A., KENYON, N. H., MINERT, J., RUMOHR, J., and WERNER, F. (1998), *The Norwegian-Greenland Sea Continental Margins: Morphology and Late Quaternary Sedimentary Processes and Environment,* Quaternary Science Review *17,* 273–302.

WILSON, R. C. and KEEFER, D. K. (1983), *Dynamic Analysis of a Slope Failure from the 1979 Coyote Lake, California, Earthquake,* Bull. Seismol. Soc. Am. *23,* 863–877.